Cell. Mol. Life Sci. (2012) 69:4215–4228
DOI 10.1007/s00018-012-1140-0

Cellular and Molecular Life Sciences

RESEARCH ARTICLE

NLRP3 inflammasome activation in macrophage cell lines by prion protein fibrils as the source of IL-1β and neuronal toxicity

Iva Hafner-Bratkovič · Mojca Benčina · Katherine A. Fitzgerald · Douglas Golenbock · Roman Jerala

Received: 16 March 2012 / Revised: 1 August 2012 / Accepted: 13 August 2012 / Published online: 29 August 2012

Abstract Prion diseases are fatal transmissible neurodegenerative diseases, characterized by aggregation of the pathological form of prion protein, spongiform degeneration, and neuronal loss, and activation of astrocytes and microglia. Microglia can clear prion plaques, but on the other hand cause neuronal death via release of neurotoxic species. Elevated expression of the proinflammatory cytokine IL-1β has been observed in brains affected by several prion diseases, and IL-1R-deficiency significantly prolonged the onset of the neurodegeneration in mice. We show that microglial cells stimulated by prion protein (PrP) fibrils induced neuronal toxicity. Microglia and macrophages release IL-1β upon stimulation by PrP fibrils, which depends on the NLRP3 inflammasome. Activation of NLRP3 inflammasome by PrP fibrils requires depletion of intracellular K^+, and requires phagocytosis of PrP fibrils and consecutive lysosome destabilization. Among the well-defined molecular forms of PrP, the strongest NLRP3 activation was observed by fibrils, followed by aggregates, while neither native monomeric nor oligomeric PrP were able to activate the NLRP3 inflammasome. Our results together with previous studies on IL-1R-deficient mice suggest the IL-1 signaling pathway as the perspective target for the therapy of prion disease.

Keywords Prions · Amyloid · Inflammasome · NLRP3 · IL-1β · Neuroinflammation

Abbreviations

ASC	Apoptosis-associated speck-like protein
NLRP3	NACHT, LRR, and PYD domains-containing protein 3
PrP	Prion protein

Introduction

Prion diseases are lethal neurodegenerative diseases affecting human and other mammalian species. These diseases include scrapie in sheep, bovine spongiform encephalopathy in cow, and chronic wasting disease in deer and elk. Transmission of scrapie to mice led to the development of many experimental prion strains differing in incubation period and profiles of pathological lesions in the central nervous system. Human prion diseases can be acquired, sporadic, or genetic. Creutzfeld-Jakob disease (CJD) is the most common type with an incidence about one per million per year. Hereditary forms include familial CJD, fatal familial insomnia and Gerstmann-Sträussler-Scheinker syndrome, and originate from mutations in the gene encoding the prion protein. Acquired human prion diseases

Electronic supplementary material The online version of this article (doi:10.1007/s00018-012-1140-0) contains supplementary material, which is available to authorized users.

I. Hafner-Bratkovič · M. Benčina · R. Jerala (✉)
Department of Biotechnology, National Institute of Chemistry, Hajdrihova 19, 1000 Ljubljana, Slovenia
e-mail: roman.jerala@ki.si

M. Benčina · R. Jerala
EN→FIST Centre of Excellence, Dunajska 156, 1000 Ljubljana, Slovenia

K. A. Fitzgerald · D. Golenbock
Department of Medicine, Division of Infectious Diseases and Immunology, University of Massachusetts Medical School, 55 Lake Avenue North, 01605 Worcester, MA, USA

R. Jerala
Faculty of Chemistry and Chemical Technology, University of Ljubljana, Aškerčeva 5, Ljubljana, Slovenia

are kuru, new variant CJD (due to ingestion of contaminated beef) and iatrogenic forms. Prion diseases are enigmatic since the infectious agent is composed primarily of an abnormal form of prion protein, PrP^{Sc} [1]. During prion disease, normal prion protein PrP^{c} converts to protease-resistant PrP^{Sc}. The three-dimensional structure of PrP^{Sc} has not been resolved, but is in contrast to the native predominantly α-helical PrP^{c}, enriched in β-secondary structure, and forms amyloid fibrils. The major characteristics of prion diseases revealed by post mortem analysis of human brain sections are spongiform degeneration of neurons, neuronal loss, intense reactive astrocytosis, and accumulation of amyloid plaques composed of PrP^{Sc} [2]. Analysis of brains of scrapie-infected mice also revealed recruitment and activation of microglia, which are associated with PrP^{Sc} deposits [3, 4]. Activation of microglia precedes the onset of the disease and coincides with increased deposition of PrP^{Sc} [5]. Activated astrocytes and microglia release proinflammatory cytokines and neurotoxic agents such as NO, free radicals, and glutamate [6]. The proinflammatory cytokine IL-1β mRNA is upregulated more than 20-fold in the prion-infected microglia in comparison to non-infected control [7]. IL-1β is also released from astrocytes exposed to infectious brain homogenate [8]. The incubation period upon infection with two different prion strains is increased in IL-1R-deficient mice, suggesting that IL-1 plays an important role in the disease progression [9, 10]. Interestingly, in ME7 prion strain, the expression of IL-1β is low, but is exacerbated upon LPS activation [11]. Combrinck and co-workers proposed that, in chronic inflammatory neurodegenerative diseases, microglia are in the primed state and respond to peripheral infection by increased IL-1β production [11] and increased neuronal death [12].

Pro-IL-1β transcription is initiated upon NF-κB activation; however, the second trigger is required for the release of IL-1β. The active form IL-1β is produced by proteolysis of its precursor form by an intracellular protein complex called the inflammasome [13]. The most investigated NLRP3 inflammasome is composed of a sensor NLRP3 (NACHT, LRR, and PYD domains-containing protein 3), an adaptor apoptosis-associated speck-like protein (ASC), and a pro-caspase-1. Upon activation, inflammasomes self-assemble, which leads to the autoactivation of pro-caspase-1. The active caspase-1 in turn cleaves and activates pro-IL-1β. Very different molecular instigators have been shown to activate NLRP3 inflammasome: ATP, microbial pore-forming toxins [14, 15], serum amyloid A [16], and schistosomal egg antigens [17], but also aggregates such as uric acid crystals [18], silica [19, 20], cholesterol crystals [21], and asbestos fibres [19].

Halle and co-workers showed that the NLRP3 inflammasome is triggered by aggregated Aβ (1–42), which is the main component of senile plaques in Alzheimer's disease [22]. This motivated us to explore if and which forms of prion protein (PrP) could activate the NLRP3 inflammasome. We demonstrate that fibrils induce NF-κB and thus provide the priming signal for the production of the pro-IL-1β and NLRP3. We also show that PrP fibrils trigger NLRP3 inflammasome assembly, which can be inhibited by inhibitors of K^+ efflux and phagocytosis. We further show that PrP fibrils are the most potent activator of the NLRP3 inflammasome, whereas oligomers and monomeric native forms do not activate inflammasomes at all. We also demonstrate that activated microglia contribute to neuronal death and suggest that in prion diseases the primed state of microglia actually occurs as a consequence of the activation of the NLRP3 inflammasome, making the microglia and brain tissue sensitive to the inflammatory signals that lead to activation of NF-κB and production of pro-IL-1β.

Materials and methods

Materials

Z-YVAD-FMK was from Biovision. All other chemicals (if not specified otherwise in the text) were from Sigma.

α-PrP isolation and refolding

Mouse prion protein was produced in bacteria in the form of inclusion bodies and refolded on a Ni^{2+} NTA column (Quiagen) by gradual decrease of guanidine hydrochloride and β-mercaptoethanol concentration to 0 M as previously described [23–27], with an additional step of thorough washing with 60 % isopropanol to remove LPS [28] before elution with 0.5 M imidazole, pH 5.8. The content of LPS as determined by LAL test (Lonza) was less than 0.15 ng/mg of protein.

Preparation of other forms of prion protein and characterization

The amyloid PrP fibrils were produced by shaking denatured mouse PrP in 1 M guanidine hydrochloride and 3 M urea in PBS pH 6.8 at protein concentrations 154 μM at 37 °C in a microtiter plate-format [25, 29]. Formation of fibrils was followed by an amyloid specific dye Thioflavin T. The PrP oligomer form was prepared by diluting protein from 10 to 5 M urea, 0.2 M NaCl, 20 mM sodium acetate buffer, pH 4.0, and incubating overnight at room temperature [30]. To determine the yield of conversion, the conversion reaction was analyzed by gel filtration on Biosep-sec-s 4000 (Phenomenex) column [23]. Dialyzed methanol-precipitated PrP served as amorphous PrP aggregates. Precipitates were observed under the confocal microscope (bright field) Leica

TCS SP5. Prior to characterization and cell culture assays, fibrils and oligomers were dialyzed against PBS. PrP 105–125 fibrils were prepared by dissolving synthetic peptide (Keck Biotechnology) in LPS-free PBS and shaking overnight at 37 °C. Formation of fibrils was followed by Thioflavin T.

Circular dichroism

Far-UV CD spectra were recorded on an Applied Photophysics Chirascan Spectropolarimeter between 190 and 250 nm in a 1-mm path length cuvette at a protein concentration of 0.1 mg/ml.

Atomic force microscopy

To observe fibrils, oligomers, and monomeric α-PrP by atomic force microscopy, a drop of protein sample (diluted to 0.22 μM) was applied to freshly cleaved mica (Ted Pella) and left to adsorb for 5 min, after which it was washed twice with filtered Milli-Q water and dried under nitrogen. Samples were observed by Agilent Technologies 5500 Scanning Probe Microscope operating in acoustic alternating current mode utilizing silicon cantilevers (Arrow-NCR; NanoWorld) [24, 25].

Cell cultures

Preparation of immortalized microglial cells from caspase-1-deficient and IL-1R-deficient mice and macrophages from NLRP3-deficient mice and ASC-deficient mice and corresponding wild-type control (C57BL/6) was described by Halle et al. [22] and Hornung et al. [20]. Immortalized microglial cells, immortalized macrophages, and RAW-Blue cells were cultured in DMEM supplemented with 10 % FBS. CAD cell line [31] was cultured in Optimem medium supplemented with 10 % FBS. All cell culture supplies were from Invitrogen.

IL-1β ELISA

All experiments were performed in serum-free DMEM. Cells were primed with ultra-pure LPS (100 ng/ml; Invivogen) for 5–6 h after which medium was removed and different concentrations of activators in DMEM were added and left overnight (or 1 h for ATP). Potential inhibitors were added 1 h before the addition of stimulators. The concentration of secreted IL-1β was measured by ELISA (e-Bioscience) according to manufacturer's instructions.

Western blotting

Experiments were performed as for measuring IL-1β ELISA, with exception that stimulation was finished after 3 h. Methanol precipitation was used to precipitate proteins from cell culture media. Cells were washed twice with cold PBS and lysed. Protein concentration in the cell lysate was measured with BCA. Proteins were separated on 15 % SDS-PAGE gels, blotted onto the nitrocellulose membrane (GE Healthcare), and detected with appropriate primary and secondary antibodies [for detection of IL-1β: B122 and Goat anti-Armenian hamster IgG-HRP (Santa Cruz); for detection of caspase-1: M-20 (Santa Cruz), and goat anti-mouse HRP-conjugated secondary antibodies from Jackson Immunoresearch]. SuperSignal West Femto Chemiluminescent Substrate (Thermo Scientific) was used for detection of HRP-labeled bands.

Caspase-1 activation

Activation of caspase-1 was followed under the confocal microscope (Leica) and flow cytometer Cyflow (Partec) using Fluorochrome Inhibitor of Caspase 1 kit (Immunochemistry Technologies) according to the manufacturer's instructions.

Confocal microscopy

A Leica TCS SP5 laser scanning microscope mounted on a Leica DMI 6000 CS inverted microscope (Leica Microsystems, Germany) with an HCX plan apo ×63 (NA 1.4) oil immersion objective was used for imaging. For acquisition and images processing, Leica LAS AF software was used. For all confocal microscopy experiments, cells were seeded into μ-Slides (Ibidi).

To follow phagocytosis of fibrils conjugated with Alexa 633, fibrils were first labeled with Alexa Fluor 633 (Invitrogen) according to the manufacturer's instructions. Macrophages were primed with LPS (100 ng/ml), and fibrils-Alexa 633 conjugate was added several hours prior staining with Cholera toxin subunit B Alexa 488 conjugate (1 mg/l) (Invitrogen) and Hoechst (1 mg/l). Cells were washed and fixed with 4 % PFA. To follow the effect of fibrils upon lysosomes, Oregon green dextran (10 mg/l) or DQ-ovabumin (10 mg/l) (both from Invitrogen) were added to primed macrophages together with unlabeled fibrils after several hours prior staining with Cholera toxin subunit B Alexa 555 conjugate, and Hoechst.

To assess microglia-induced neurotoxicity of PrP fibrils, the experiment was performed as described previously [22]. Mouse neuronal cells CAD [31] were first differentiated by withdrawal of serum for 2 days. Microglial cells were added, primed with LPS, and stimulated with fibrils. The co-culture was grown in serum-free media for 3 days. Next, cells were fixed with 4 % PFA and permeabilized with 0.01 % Triton X-100, and stained for neuron-specific marker III β-tubulin [primary antibody (Cell Signaling

Technologies), secondary antibodies Cy2-labeled goat anti-mouse polyclonal antibodies (Abcam), and with anti-mouse CD11b eFlour 650 NC antibodies (eBioscience)] and observed under confocal microscope.

A 405-nm laser line of a 20-mW diode laser was used for Hoechst excitation and emitted light was detected between 430 and 490 nm. A 488- to 514-nm laser line of 100-mW argon laser with 3 % laser power was used for Oregon green dextran, Cholera toxin subunit B Alexa 488 conjugate, DQ-ovabumin, and Cy2-labeled goat anti-mouse polyclonal antibodies, and emitted light was detected between 500 and 560 nm or 525 and 580 nm. A 543-nm laser line of 1.5-m mW HeNe laser was used for excitation of Cholera toxin subunit B Alexa 555 conjugate, and emitted light was detected in a window between 560 and 630 nm. A 633-nm laser line of 10-m mW HeNe laser was used for excitation of fibrils-Alexa 633 conjugate and anti-mouse CD11b eFlour 650 NC antibodies, and emitted light was detected in a window between 640 and 700 nm.

Post-acquisition processing and the size analysis of DQ-OVA positive lysosomes were performed with image analysis software ImageJ, as described by Glunde et al. [32]. For analysis of DQ-OVA positive lysosomes, lysosomal ROIs with areas larger than 0.6 μm^2 were selected. On average, 50 cells from two independent experiments were analyzed.

Acridine orange stain for flow cytometry

Cells were stained for 15 min with acridine orange in PBS (10 μg/ml), after which cells were washed twice with PBS and medium containing LPS and LPS plus various forms of PrP was added. Several hours afterwards, cells were washed several times and analyzed by flow cytometry.

Microglia/neuron co-culture experiment to assess the number of live neurons

Mouse neuronal cells CAD [31] were seeded into 24-well microtiter plates and first differentiated by withdrawal of serum for 2 days. Polycarbonate tissue culture inserts (0.4 μm pore size; Nunc) were inserted into the wells. Microglial cells were seeded into half of the inserts. After 4 h, medium in microtiter wells was replaced by 250 μl of serum-free low glucose DMEM (Gibco), and stimulators (100 ng/ml LPS or LPS + 10 μM fibrils, 500 μl) were added into culture inserts. After 2 days culture, inserts were discarded and cells in microtiter plates (neurons) were counted with addition of trypan blue to allow counting of live cells.

NO assay

After priming with interferon-γ for 1 h, different concentrations of PrP 105-125 fibrils were added and left overnight. Nitric oxide production was measured by Griess reaction.

NF-κB activity

Raw-Blue cells (Invivogen) were seeded into wells containing different concentrations of PrP 105–125 fibrils in DMEM not supplemented with FBS. The next day, alkaline phosphatase in cell culture medium was analyzed colorimetrically with Quanti-Blue assay (InvivoGen).

Statistical analysis

Unpaired two-tailed *t* test was used for pairwise comparison.

Results

PrP fibril-activated microglia are neurotoxic

One of the major characteristics of prion diseases is reactive gliosis. Activated microglial cells gather around prion plaques in diseased brain tissue [3, 4]. PrP^{Sc} was also found in microglial cells [33]. While fibrils by themselves can be toxic to neurons [34], we wanted to assess whether the fibril toxicity is increased upon activation of microglial cells. Neurons were cultured either alone (Fig. 1a, upper row) or in the co-culture with microglia (Fig. 1a, bottom row) and primed with LPS (Fig. 1a, left) or primed with LPS and activated with PrP fibrils (Fig. 1a, right). Interestingly, we did not observe any direct fibril toxicity to neurons at the concentrations used (Fig. 1a, b); however, it is possible that this is due to the immortalized neuronal cell line used. Some other neuronal cell lines were previously shown to be less sensitive to direct effects of PrP fibrils [34]. An immortalized microglial cell line has been previously characterized [22] and shown to respond to Aβ aggregates as do primary microglial cells. The number of neurons decreased when the co-culture was stimulated with PrP fibrils (Fig. 1a, b). We also show that microglial cells upon priming with IFN-γ and activation with synthetic PrP 105-125 fibrils release free radical NO similar to treatment with LPS or zymosan (Fig. 1c). This demonstrates that PrP fibrils are able to activate microglia to release neurotoxic species, such as NO, which induces neuronal death.

IL-1β is released from macrophages and microglia activated by PrP fibrils

Since IL-1β is one of the major proinflammatory cytokines upregulated in prion disease [7], we investigated whether PrP fibrils are able to induce IL-1β secretion. Release of

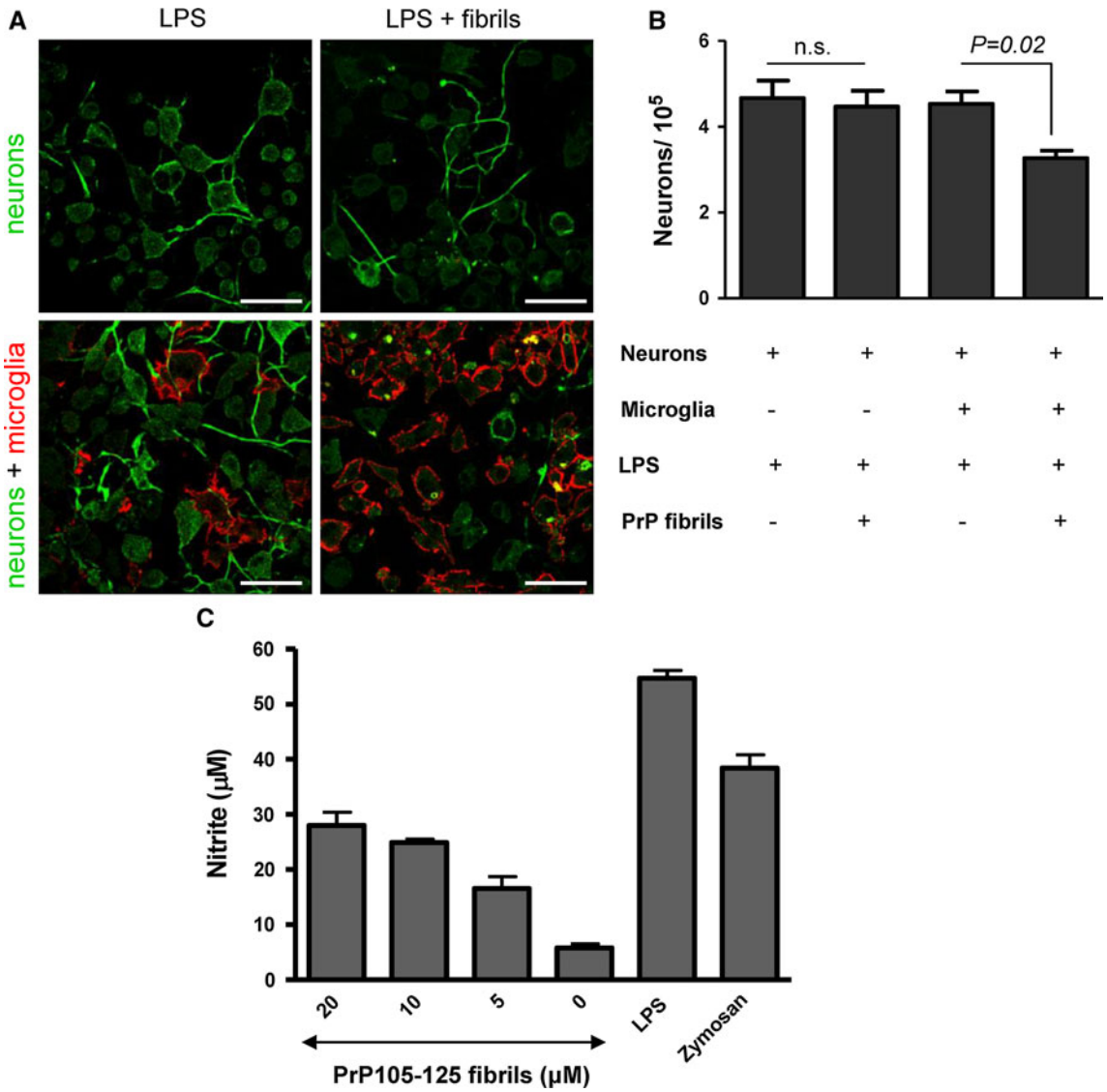

Fig. 1 PrP fibril-activated microglial cells release neurotoxic species. **a** Neurons were cultured either alone (*top row*) or in the presence of microglia (*bottom row*) and stimulated by LPS (100 ng/ml, *left*) or LPS and fibrils (8 μM) (*right*). Neurons were labeled by antibodies against neuron specific β-tubulin and Cy2-labeled secondary antibodies. Microglia were detected by eFlour 650 NC-labeled antibodies against CD11b. *Scale bar* 50 μm. **b** Neurons were cultured alone or with microglia in cell culture inserts. LPS was added to all culture inserts. After 2 days incubation with or without fibrils (10 μM), culture inserts were discarded and neurons attached to microtiter plate wells were counted by trypan blue exclusion test. Total count of live cells is represented. **c** Microglia secrete NO upon stimulation with fibrils from prion protein peptide 105–125 comparable to known stimuli LPS (100 ng/ml) and zymosan (10 μg/ml). The concentration corresponds to the initial amount of monomeric peptide prior fibrillization. Representative examples of 2 (**b**) and 3 (**c**) independent experiments are shown. *Error bars* SD of triplicate wells (**b**, **c**)

IL-1β by LPS-primed macrophages and microglia into the cell culture medium was monitored, demonstrating that PrP fibrils are indeed able to induce IL-1β production (Fig. 2a, b). We detected mature IL-1β (p17) in cell culture medium of activated macrophages by western blotting, while no IL-1β was processed from unprimed or primed-only macrophages (Fig. 2c). As previously observed for maturation of IL-1β by uric acid crystals [18], the amount of pro-IL-1β in the cell decreases with increased release of the active form (Fig. 2c). To ensure strong activation of NF-κB and thus expression of pro-IL-1β, cells were primed with LPS. In our experimental setup, we observed no IL-1β release due to PrP fibrils in the absence of priming (Fig. 2a, b). Nevertheless, several studies have shown that amyloid fibrils are able to induce NF-κB [35–37]. To test whether the NF-κB priming could be facilitated through PrP fibrils, we subjected indicator RAW-Blue cell line to synthetic LPS-free PrP 105–125 fibrils. RAW-Blue cell line expresses NF-κB/AP-1-inducible secreted embryonic alkaline phosphatase. Indeed, PrP 105–125 fibrils induced

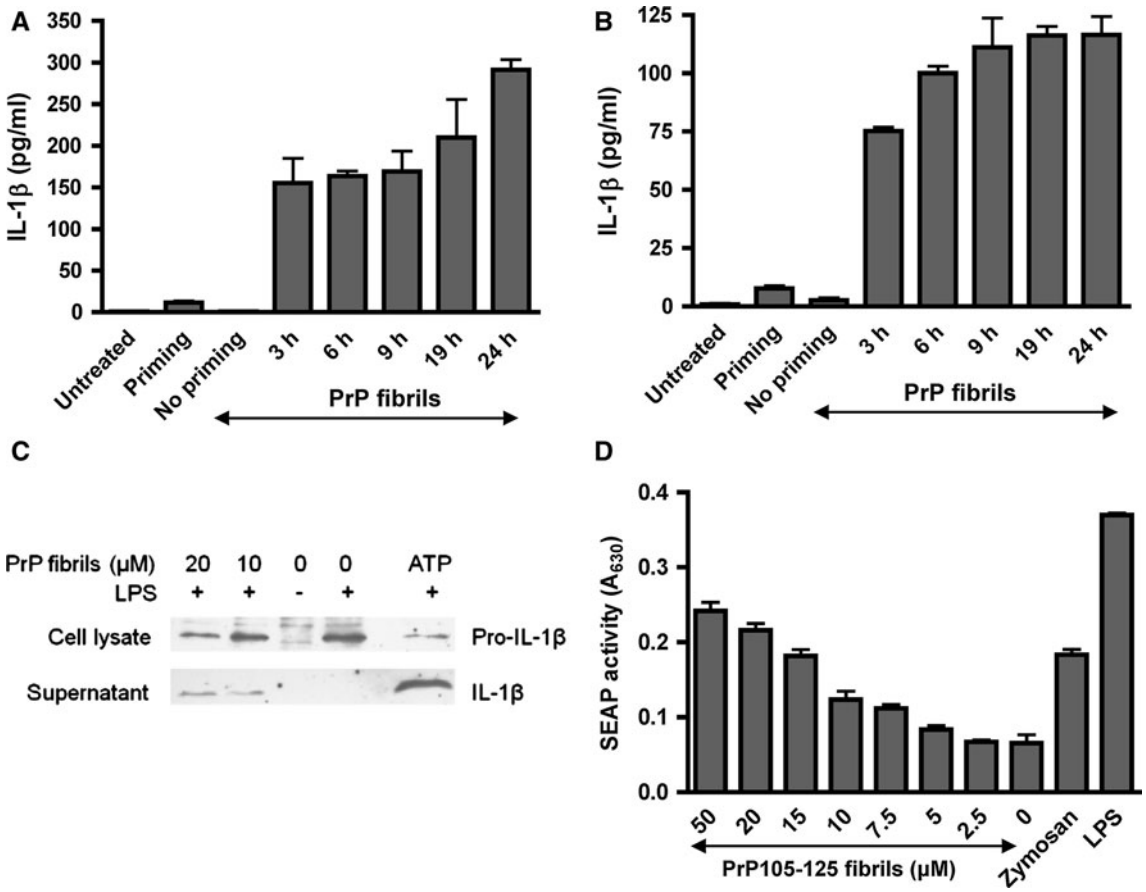

Fig. 2 Macrophages and microglia release IL-1β upon stimulation with PrP fibrils. Immortalized macrophages (**a**) and microglia (**b**) were primed for 6 h with LPS, after which fibrils (10 μM) were added and IL-1β release was followed with time with IL-1β ELISA. Cell culture medium of untreated, primed only and unprimed cells stimulated with fibrils was assayed 19 h post stimulation with fibrils. *Error bars* SD of triplicate wells. **c** Mature IL-1β (p17) is secreted into the cell culture medium (SN) by macrophages after stimulation by PrP fibrils and ATP (5 mM). Pro-IL-1β is followed in cell lysate (CL). Representative western blots of 4 experiments are shown. **d** PrP 105–125 fibrils are able to activate NF-κB pathway similarly to LPS (10 ng/ml) and zymosan (1 μg/ml). The concentration corresponds to the initial amount of monomeric peptide prior fibrillization. Representative examples of 4 experiments are shown. *Error bars* SD of triplicate wells

concentration-dependent secretion of alkaline phosphatase. Recently, Zhao and co-workers [38] reported that aggregated PrP 105–125 via integrin $\alpha5\beta1$ upregulated expression of NLRP3, which could be decreased by inhibitors of NF-κB and ROS [39]. All these results show that PrP fibrils are able to induce IL-1β release, but can also provide the signal for NF-κB activation, necessary for expression of pro-IL-1β and NLRP3.

PrP fibrils activate caspase-1

Caspase-1 is the main activator of IL-1β maturation in mononuclear phagocytes. To follow the activation of caspase-1, we used fluorescent covalent inhibitor, which binds only to active caspase-1 but not to procaspase-1. We analyzed the activation of caspase-1 in primed and PrP fibril-activated macrophages as detected by confocal microscopy (Fig. 3a) and flow cytometry (Fig. 3b). Active caspase-1 subunit p10 was also detected by western blotting in the cell culture medium upon activation by fibrils and in a positive control, stimulated with ATP (Fig. 3c). There was no caspase-1 activation in unprimed or LPS primed-only cells (Fig. 3c). Further, immortalized microglial cells from the caspase-1-deficient, IL-1R-deficient, and matching wild-type mice were treated with PrP fibrils. Caspase-1-deficient microglia failed to secrete IL-1β while wild-type microglia dose-dependently released IL-1β (Fig. 3d). IL-1R-deficient microglia efficiently released IL-1β, demonstrating that PrP fibril-induced secretion of IL-1β is independent of IL-1R signaling (Fig. 3d). Additionally, caspase-1 inhibitor Z-YVAD-FMK inhibits maturation of IL-1β (Fig. 3e). We thereby demonstrated that PrP fibrils induced maturation of IL-1β in a manner that depends on caspase-1 activity.

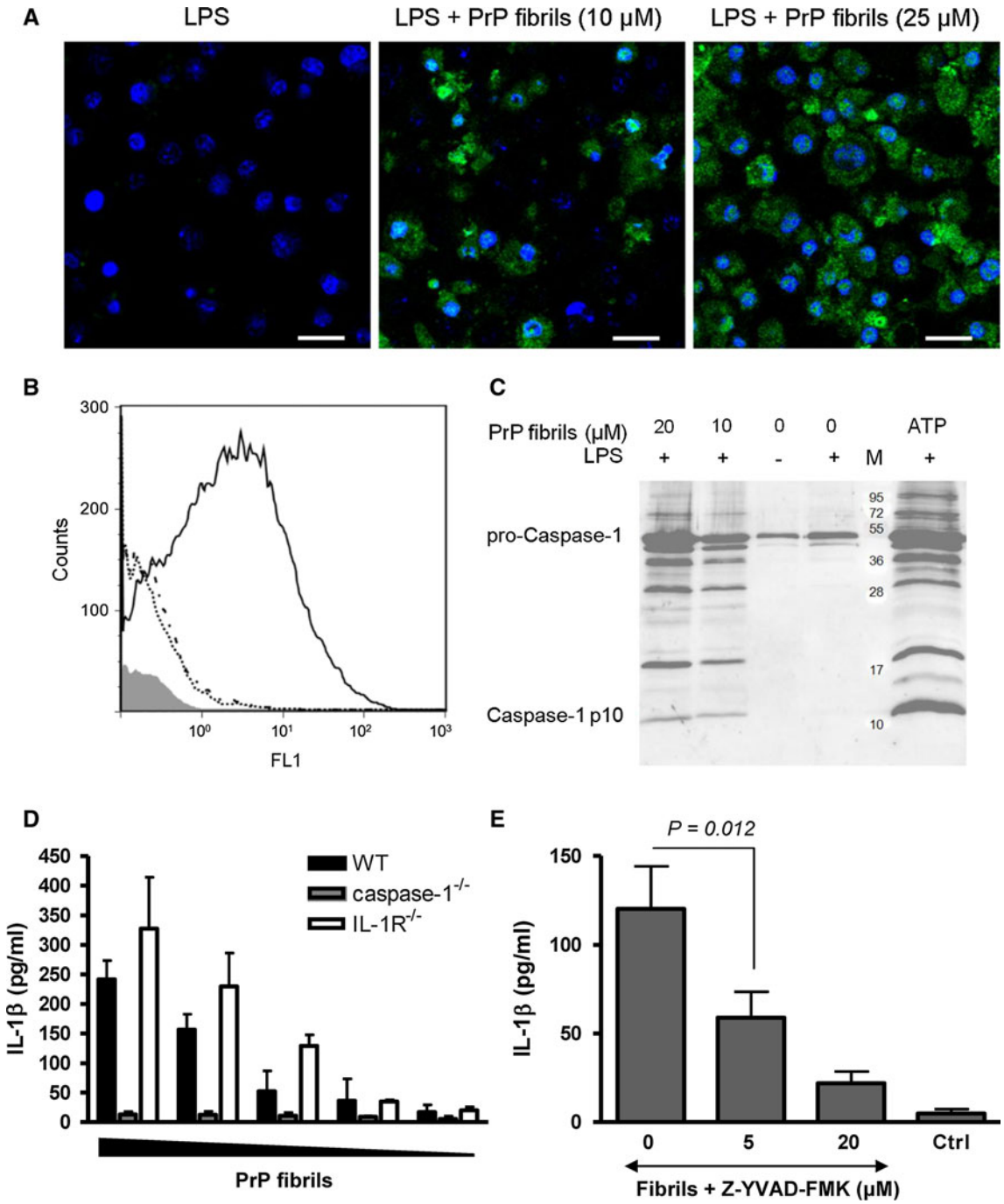

Fig. 3 PrP fibrils activate caspase-1. Fluorescent inhibitor of caspase-1 was used to detect caspase-1 activation by PrP fibrils by confocal microscopy (**a**) or by flow cytometry (**b**). **a** LPS-primed immortalized macrophages were treated with fibrils (10 and 25 μM). *Scale bar* 25 μm. **b** Histogram of fibril-treated (10 μM) (*full line*), primed-only (*dash/dotted line*) and untreated macrophages (*dotted line*). The histogram of unlabeled cells (without fluorescent inhibitor of caspase-1) is shown in *gray*. **c** Cleaved caspase-1 (p10) was detected in cell culture media of macrophages stimulated by PrP fibrils and ATP (5 mM). No p10 is detected in untreated or primed only samples. **d** IL-1β processing induced by PrP fibrils (20, 10, 7, 5, and 3 μM of monomeric PrP in the fibrillar form) in immortalized microglia, deficient in caspase-1 and IL-1R and corresponding wild-type microglia was followed by IL-1β ELISA. Secreted IL-1β concentration was corrected for background (priming only). **e** IL-1β maturation by PrP fibrils (8.5 μM) in macrophages is decreased upon addition of caspase-1 inhibitor Z-YVAD-FMK. Representative examples of 3 (**a**), 2 (**b**), 3 (**c**, **d**, **e**) independent experiments are shown. *Error bars* SD of duplicate (**d**) and triplicate (**e**) wells

PrP fibrils activate NLRP3 inflammasome

Caspase-1 is activated by several distinct NLR or PYHIN containing inflammasomes. Since several other particulate triggers [18–20, 22] were shown to activate the NLRP3 inflammasome, we wanted to investigate if the same mechanism is also responsible for activation of caspase-1 by aggregated PrP, the hallmark of prion diseases. We show that production of IL-1β induced by PrP fibrils is abrogated in macrophages deficient in NLRP3 or ASC, while wild-type macrophages are efficiently and dose-dependently activated by PrP fibrils (Fig. 4a). The inability of macrophages deficient in NLRP3 or the signaling adaptor ASC to release IL-1β demonstrates that PrP fibrils induce activation of the NLRP3 inflammasome, which in turn activates caspase-1 and IL-1β.

Further, we investigated the mechanism of NLRP3 inflammasome activation by PrP fibrils. PrP fibrils could activate NLRP3 directly or indirectly through induction of other activators of the NLRP3 inflammasome. Since PrP fibrils are able to induce cell death in macrophages (Fig. S1), it is possible that dying cells could release ATP, which is a potent activator of the NLRP3 inflammasome. This is not the case, since the addition of apyrase, the ATP-hydrolyzing enzyme, had no effect on IL-1β release by PrP fibrils in contrast to the ATP-stimulated control (Fig. 4b). On the other hand, depletion of intracellular K^+ has also been described as characteristic for NLRP3 inflammasome activation [40]. Inhibition of the cytoplasmic K^+ efflux, either by the addition of KCl-conditioned media or glyburide, an inhibitor of ATP-dependent K^+ channels, decreased the activation of inflammasome by PrP fibrils (Fig. 4c), demonstrating the role of K^+ efflux in the activation.

Phagocytosis of PrP fibrils results in lysosome destabilization

To follow the fibril–macrophage interaction, PrP fibrils were fluorescently labeled, which did not affect the activation process. After several hours, the majority of macrophages contained internalized PrP fibrils (Fig. 5a). Inhibition of phagocytosis by the addition of cytochalasin D, a phagocytosis inhibitor, which blocks actin polymerization, correlated with a decrease in the inflammasome activation (Fig. 5b). This suggests that phagocytosis of PrP fibrils is necessary for the inflammasome activation as has been previously reported for several other particulate activators [19–22]. Unlabeled fibrils were added to macrophages together with DQ-ovalbumin. DQ-ovalbumin exhibits fluorescence only in compartments where proteases degrade ovalbumin, resulting in dequenching of the fluorophore. Phagocytosis of PrP fibrils induced lysosome swelling (Fig. 5c, middle), while in macrophages that were not exposed to fibrils, DQ-ovalbumin labeled small vesicles (Fig. 5c, left). Similar results were also obtained with fluorescent dextran as an alternative endosomal marker (Fig. S2). The size of DQ-ovalbumin-labeled lysosomes was measured. On average, the area of lysosome increased more than twice upon stimulation by PrP fibrils (Fig. 5c, right). To follow the lysosome integrity, we used acridine orange stain. Acridine orange bound to DNA emits green fluorescence, but when accumulated in acidic compartments, which results in dimerization, its fluorescence emission shifts into the red. The loss of red fluorescence which corresponds to the loss of intact lysosomes was observed upon addition of PrP fibrils (Fig. 5d). As in the case of silica [20] and Aβ fibrils [22], we also observed cytosolic DQ-ovalbumin staining in PrP fibril-treated macrophages (Fig. 5d, right), suggesting that ingestion of PrP fibrils led to leakage of the lysosomal content into the cytosol.

Fibrillar form is the most potent inflammasome activating molecular form of the PrP

The requirement for the type of the protein molecular assemblies that can induce NLRP3 inflammasome has so far not been well characterized by parallel testing of several isolated and well-characterized forms. We prepared and characterized several different PrP assemblies: amorphous aggregates, PrP fibrils, PrP oligomers, and monomeric PrP. Monomeric PrP has a predominantly α-helical secondary structure (Fig. S3a), while PrP fibrils as well as oligomers have an increased content of the β-secondary structure (Fig. S3b). Additionally, we also prepared PrP aggregates, which vary in size from as low as 1 to almost 100 μm, with most particles in the range of 10–20 μm (Fig. 6a, left). We show that PrP aggregates are able to activate the NLRP3 inflammasome (Fig. 6a, right). PrP fibrils are approximately 7-nm thin fibrils with lengths in the range from 100 nm to several μm (Fig. 6b, left) [25]. We demonstrated throughout this study that PrP fibrils activate the NLRP3 inflammasome. If we compare the level of secreted IL-1β, PrP fibrils are significantly more efficient in inflammasome activation than PrP aggregates (Fig. 6a, b). While the conversion efficiency to PrP fibrils is 100 % [24], the conversion efficiency to oligomers, estimated from gel filtration analysis, was ~40 % (Fig. S3c). Oligomers measure about 30 nm in diameter as estimated from AFM images (Fig. 6c). Surprisingly, oligomers did not activate the inflammasome (Fig. 6c) and neither did the native non-pathological monomeric α-PrP (Fig. 6d). In vitro-prepared PrP fibrils and oligomers morphologically correspond to PrP species found in the diseased brain. Studies using prion rods (scrapie-associated fibrils) and prion oligomers isolated from the diseased brain are limited

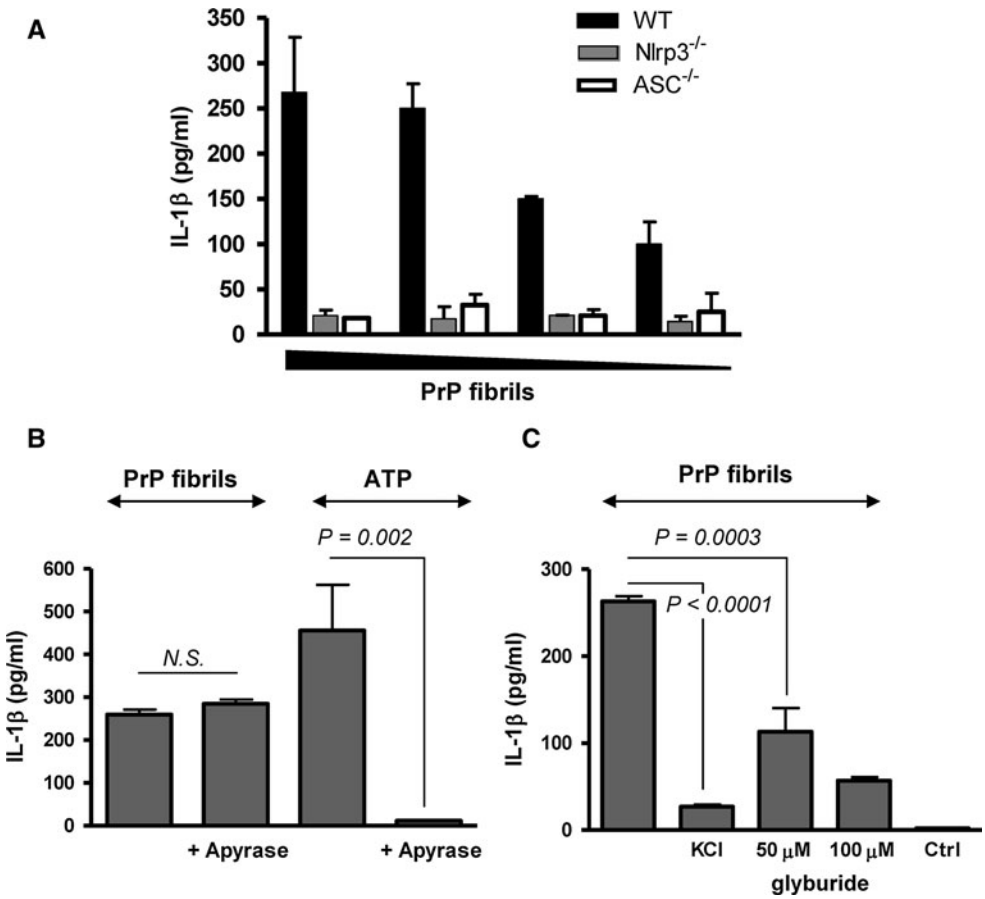

Fig. 4 Prion fibrils activate NLRP3 inflammasome. **a** Wild-type, NLRP3-deficient, and ASC-deficient macrophages were primed and stimulated with different amounts of PrP fibrils (10, 7, 5, 3 μM of monomeric PrP in the fibrillar form). Secreted IL-1β concentration was corrected for background (priming only). **b** Apyrase (0.4 U), an ATP hydrolyzing enzyme, had no affect on IL-1β release induced by PrP fibrils (8.5 μM). **c** The inhibition of K^+ efflux by addition of 130 mM KCl to medium or by glyburide inhibits IL-1β release by PrP fibrils (20 μM). Representative examples of 3 (**a**), 4(**b**, **c**) independent experiments are shown. *Error bars* SD of triplicate wells

by the amount of the isolated material, heterogeneity, and its purity, since isolates might be contaminated by other endogenous NLRP3 triggers such as nucleic acids or ATP. Our bacterially expressed PrP did not contain significant amounts of LPS. PrP fibrils, oligomers, and monomers were all prepared from the same starting material, but presented significantly different NLRP3 inflammasome activation, further supporting our conclusions that NLRP3 inflammasome activation is due to specific protein assemblies. The use of recombinant prion proteins and its converted forms is further corroborated by recent studies showing that infectious prion disease can be induced by in vitro-converted bacterially expressed PrP [41–44]. Using different, well-characterized PrP assemblies, we were able to show that NLRP3 inflammasome activation via particulate protein assemblies depends on the type of aggregate. We suggest that PrP fibrils are potent activators, since they are readily phagocytosed by macrophages, but are resistant to proteolysis and cause lysosome destabilization. Oligomers and monomeric PrP do not cause lysosome swelling and the leakage of lysosomal content into the cytosol (Fig. S4), and thus do not activate NLRP3 inflammasome.

Discussion

Prion diseases are characterized by neuroinflammation, which contributes to the loss of neurons and the decay of the cognitive functions. We have shown that PrP fibrils induce production of IL-1β through activation of the NLRP3 inflammasome. We tested several different in vitro-prepared PrP forms and showed that the larger particles (aggregates and fibrils) activate the NLRP3 inflammasome in contrast to native α-form. PrP oligomers, which have been proposed as the most infectious PrP species [45], do not activate the inflammasome. Previous studies identified Aβ fibrils [22], peptide fragments from prion protein (PrP 105–125) [39], and amylin oligomers [46] as amyloid activators of NLRP3 inflammasome. Masters and co-workers have shown that the NLRP3

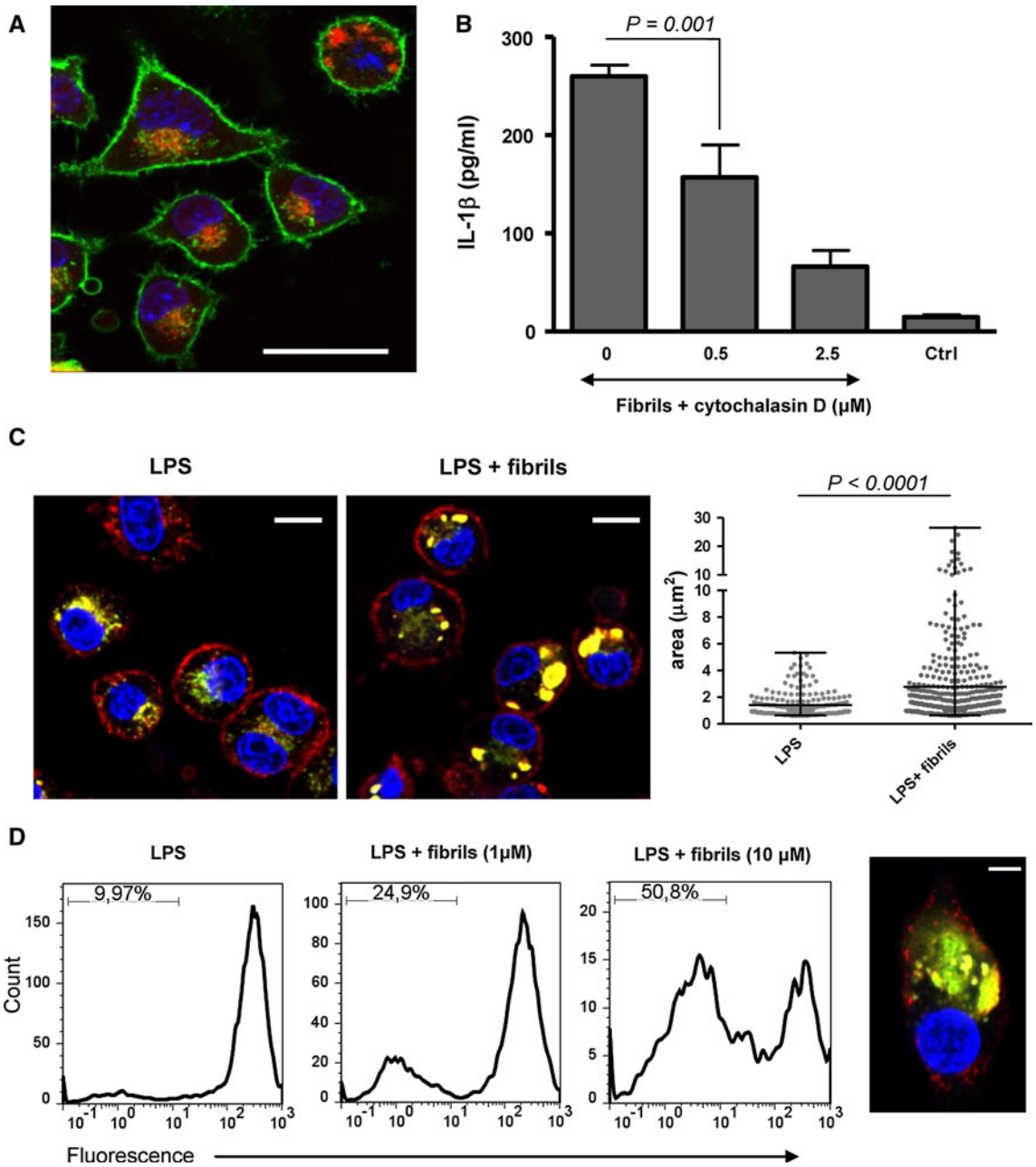

Fig. 5 Fibrils cause lysosome destabilization upon phagocytosis. **a** Alexa 633-labeled fibrils (*red*) are phagocytosed by macrophages (*green*: cholera toxin subunit B; *blue*: Hoechst). *Scale bar* 25 μm. **b** IL-1β release by PrP fibrils (8.5 μM) is decreased upon addition of phagocytosis inhibitor cytochalasin D. *Error bars* mean SD of quadruplicate wells. **c** Macrophages were incubated with unlabeled fibrils (*middle*) or without fibrils (*left*) and with DQ-ovalbumin (*red*: cholera toxin subunit B; *green*: DQ-ovalbumin; *blue*: hoechst). Lysosome swelling was observed in cells treated with PrP fibrils (*middle*). *Scale bars* 10 μm. Areas of individual lysosomes from 50 cells are depicted and show significant increase in lysosome size upon stimulation with fibrils (*right*). **d** The loss of lysosome integrity as followed by acridine orange stain increased with increasing concentrations of PrP fibrils (*left*). Response of live cells is shown. Cytosolic DQ-ovalbumin stain indicating leakage of lysosomal content into the cytosol was observed in several cells treated with PrP fibrils (*red*: cholera toxin subunit B; *green*: DQ-ovalbumin; *blue*: hoechst). *Scale bar* 5 μm (*right*). Representative examples of 2 (**a**, **c**, **d**) and 4 (**b**) experiments are shown

inflammasome is activated by amylin oligomeric fractions with molecular weight of <100 kDa [46]. We observed no activation with PrP oligomers, which are even larger than amylin oligomers (Fig. 6c). Filtering through a 200-nm filter almost completely abolished the activation by PrP fibrils (not shown), thus the mechanism of inflammasome activation by different amyloids may not be identical. Some amyloid-forming peptides are prone to aggregation,

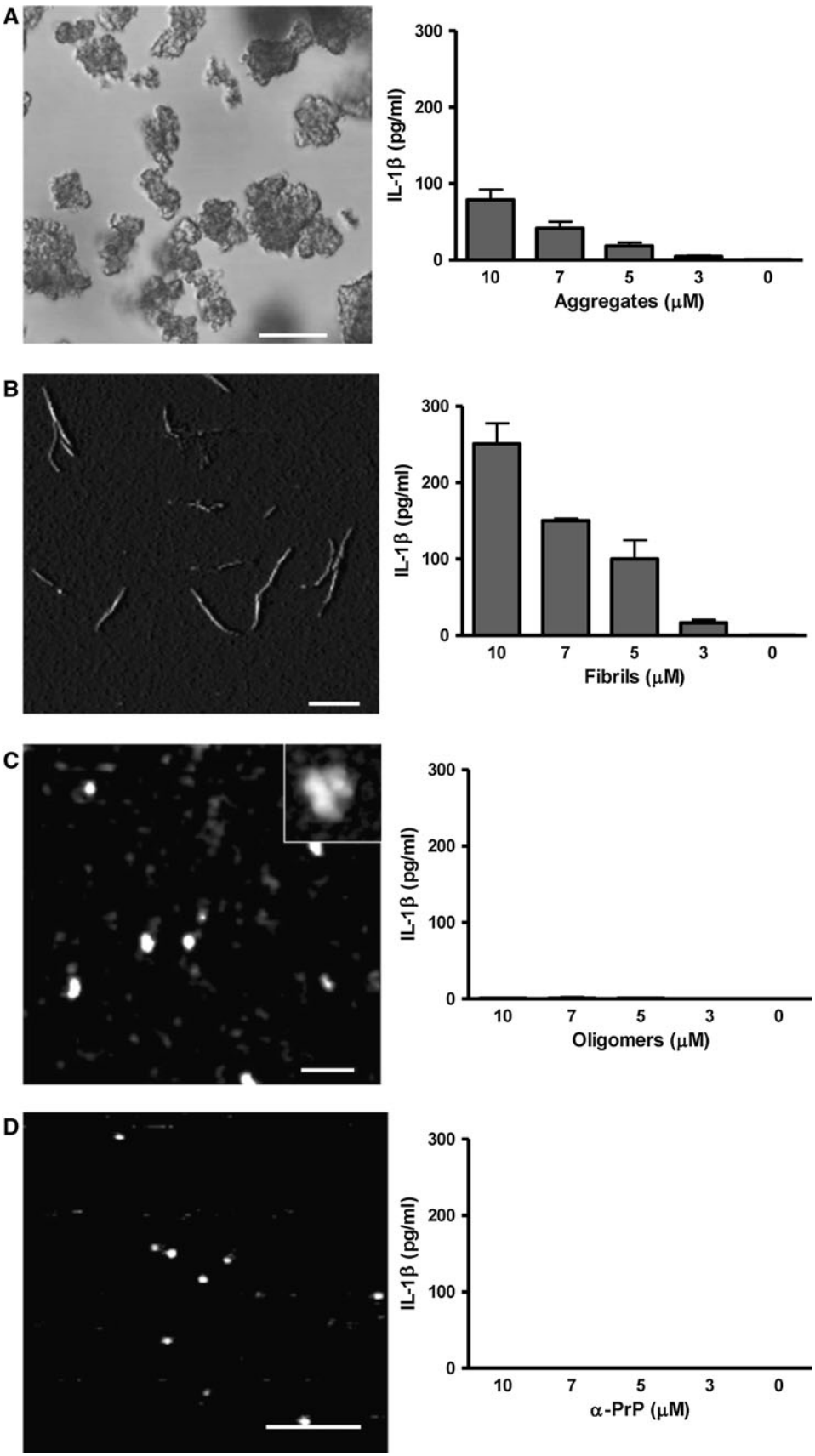

Fig. 6 Fibrils are the most potent inflammasome activators among different PrP species. **a** Aggregates, **b** fibrils, **c** oligomers, and **d** PrP monomers (α-PrP) were visualized under the confocal microscope (aggregates) or AFM and tested for their ability to induce IL-1β release by macrophages. Concentrations are the amounts of monomeric PrP in each form. Representative of three independent experiments is shown. *Error bars* SD of triplicate wells. *Scale bars* (**a**) 20 μm, (**b**) 1 μm, (**c**) 200 nm, (**d**) 100 nm

thus careful physical characterization immediately prior to cell stimulation is required in order to identify the present molecular species. The size dependence of inflammasome activation by PrP assemblies is in accordance with the activation of NLRP3 inflammasome by differently-sized polystyrene microparticles [47].

NLRP3 inflammasome activation by PrP fibrils leads to release of proinflammatory cytokine IL-1β, which signals through IL-1R. Upon activation, IL-1R recruits the intracellular adaptor MyD88. Inoculation of MyD88-deficient mice with prion strain RML demonstrated no significant delay in the incubation period [48]. However, two independent studies have reported prolonged incubation period in IL-1R-deficient mice infected by prion strains 139A and RML [9, 10], suggesting that IL-1β does participate in the pathophysiology of the disease. Schultz and co-workers showed significantly delayed activation of astrocytes and delayed accumulation of the pathological prion protein in IL-1R-deficient mice [9]. Microglia is activated by deposited amyloid, and this activation is IL-1R-independent [9], which is also supported by our experiments (Fig. 3d). Activated microglia could exert their neurotoxic effects either directly through production of NO (Fig. 1) [49] or, as proposed by Schultz et al. [9], through activation of astrocytes, which is at least partially dependent on IL-1. Activated astrocytes also secrete neurotoxic factors in vitro [50] and are able to replicate prions in vivo [51].

There are conflicting reports regarding the production of IL-1β in prion-infected brains and particular types of cells [7, 8, 52]. While PrP fibrils are able to activate NF-κB, this activation might not be sufficient to produce prominent amounts of pro-IL-1β, but could induce the primed state of microglia by activation of the NLRP3 inflammasome. IL-1β production in prion-infected tissue may be potentially enhanced in the case of an additional proinflammatory first signal, which stimulates the production of pro-IL-1β, such as, e.g., viral or bacterial infection or endogenous danger signals. In the ME7 mouse prion model, stimulation with LPS triggered a robust expression of IL-1β even by systemic i.p. administration [12], supporting the conclusion that the activation signal, provided by NLRP3 and described in this report, could be responsible for this activated phenotype of microglia. Prion strains differ, for example, in the type of PrP^{Sc} deposits and the size of the most infectious particles [53], thus it is possible that the role of NLRP3 inflammasome can vary depending on the predominant PrP^{Sc} size.

However, the role of microglia in prion disease as well as in other amyloidoses is not only harmful. Depletion of microglia resulted in increased accumulation of PrP^{Sc} [54], suggesting that microglial cells are able to decrease prion infectivity and progression of the disease by phagocytosis of PrP^{Sc}, as has been shown for macrophages in the spleen [55]. Administration of complete Freund's adjuvant to prion-infected mice increased the incubation period, possibly through activation of phagocytosis [56], further supporting the protective role of microglia. Thus, the activation of microglia is a double-edged sword, participating both in the degradation of protein amyloids and on the other hand in production of proinflammatory and neurotoxic mediators. This double role of the microglia may explain the apparent discrepancy between the results of MyD88 and IL-1R deficiency. Therefore, the indiscriminatory inhibition of innate immune response in prion diseases is not appropriate. On the other hand, specific inhibition of the inflammasome or its products that does not inhibit the phagocytosis, or perhaps at the stage when the phagocytic capacity of microglia is already overwhelmed, could be beneficial in therapy of prion disease and other amyloidoses.

Acknowledgments We would like to thank Darija Oven and Robert Bremšak for excellent technical assistance, Manuel Ritter and Clarissa Prazeres da Costa (TUM) for valuable discussions, Kurt Wüthrich for providing plasmid encoding mouse PrP ORF and Dona M. Chikaraishi for CAD cell line. This work was funded by Slovenian Research Agency (Z7-2059 to I.H.-B., P4-0176, N5-003, L4-2404 and J1-4170 to R.J.) and by NIH grant AI083713 to K.A.F.

Conflict of interest The authors declare that they have no conflict of interest.

References

1. Prusiner SB (1998) Prions. Proc Natl Acad Sci USA 95(23): 13363–13383
2. Budka H, Aguzzi A, Brown P, Brucher JM, Bugiani O, Gullotta F, Haltia M, Hauw JJ, Ironside JW, Jellinger K et al (1995) Neuropathological diagnostic criteria for Creutzfeldt-Jakob disease (CJD) and other human spongiform encephalopathies (prion diseases). Brain Pathol 5(4):459–466
3. Williams AE, Lawson LJ, Perry VH, Fraser H (1994) Characterization of the microglial response in murine scrapie. Neuropathol Appl Neurobiol 20(1):47–55
4. Betmouni S, Perry VH, Gordon JL (1996) Evidence for an early inflammatory response in the central nervous system of mice with scrapie. Neuroscience 74(1):1–5
5. Giese A, Brown DR, Groschup MH, Feldmann C, Haist I, Kretzschmar HA (1998) Role of microglia in neuronal cell death in prion disease. Brain Pathol 8(3):449–457
6. Suzumura A, Takeuchi H, Zhang G, Kuno R, Mizuno T (2006) Roles of glia-derived cytokines on neuronal degeneration and regeneration. Ann NY Acad Sci 1088:219–229
7. Baker CA, Manuelidis L (2003) Unique inflammatory RNA profiles of microglia in Creutzfeldt-Jakob disease. Proc Natl Acad Sci USA 100(2):675–679
8. Tribouillard-Tanvier D, Striebel JF, Peterson KE, Chesebro B (2009) Analysis of protein levels of 24 cytokines in scrapie agent-infected brain and glial cell cultures from mice differing in prion protein expression levels. J Virol 83(21):11244–11253
9. Schultz J, Schwarz A, Neidhold S, Burwinkel M, Riemer C, Simon D, Kopf M, Otto M, Baier M (2004) Role of interleukin-1

in prion disease-associated astrocyte activation. Am J Pathol 165(2):671–678
10. Tamguney G, Giles K, Glidden DV, Lessard P, Wille H, Tremblay P, Groth DF, Yehiely F, Korth C, Moore RC, Tatzelt J, Rubinstein E, Boucheix C, Yang X, Stanley P, Lisanti MP, Dwek RA, Rudd PM, Moskovitz J, Epstein CJ, Cruz TD, Kuziel WA, Maeda N, Sap J, Ashe KH, Carlson GA, Tesseur I, Wyss-Coray T, Mucke L, Weisgraber KH, Mahley RW, Cohen FE, Prusiner SB (2008) Genes contributing to prion pathogenesis. J Gen Virol 89(Pt 7):1777–1788
11. Combrinck MI, Perry VH, Cunningham C (2002) Peripheral infection evokes exaggerated sickness behaviour in pre-clinical murine prion disease. Neuroscience 112(1):7–11
12. Cunningham C, Wilcockson DC, Campion S, Lunnon K, Perry VH (2005) Central and systemic endotoxin challenges exacerbate the local inflammatory response and increase neuronal death during chronic neurodegeneration. J Neurosci 25(40):9275–9284
13. Petrilli V, Dostert C, Muruve DA, Tschopp J (2007) The inflammasome: a danger sensing complex triggering innate immunity. Curr Opin Immunol 19(6):615–622
14. Mariathasan S, Weiss DS, Newton K, McBride J, O'Rourke K, Roose-Girma M, Lee WP, Weinrauch Y, Monack DM, Dixit VM (2006) Cryopyrin activates the inflammasome in response to toxins and ATP. Nature 440(7081):228–232
15. Gurcel L, Abrami L, Girardin S, Tschopp J, van der Goot FG (2006) Caspase-1 activation of lipid metabolic pathways in response to bacterial pore-forming toxins promotes cell survival. Cell 126(6):1135–1145
16. Niemi K, Teirila L, Lappalainen J, Rajamaki K, Baumann MH, Oorni K, Wolff H, Kovanen PT, Matikainen S, Eklund KK (2011) Serum amyloid A activates the NLRP3 inflammasome via P2X7 receptor and a cathepsin B-sensitive pathway. J Immunol 186(11):6119–6128
17. Ritter M, Gross O, Kays S, Ruland J, Nimmerjahn F, Saijo S, Tschopp J, Layland LE, Prazeres da Costa C (2010) Schistosoma mansoni triggers Dectin-2, which activates the Nlrp3 inflammasome and alters adaptive immune responses. Proc Natl Acad Sci USA 107(47):20459–20464
18. Martinon F, Petrilli V, Mayor A, Tardivel A, Tschopp J (2006) Gout-associated uric acid crystals activate the NALP3 inflammasome. Nature 440(7081):237–241
19. Dostert C, Petrilli V, Van Bruggen R, Steele C, Mossman BT, Tschopp J (2008) Innate immune activation through Nalp3 inflammasome sensing of asbestos and silica. Science 320(5876): 674–677
20. Hornung V, Bauernfeind F, Halle A, Samstad EO, Kono H, Rock KL, Fitzgerald KA, Latz E (2008) Silica crystals and aluminum salts activate the NALP3 inflammasome through phagosomal destabilization. Nat Immunol 9(8):847–856
21. Duewell P, Kono H, Rayner KJ, Sirois CM, Vladimer G, Bauernfeind FG, Abela GS, Franchi L, Nunez G, Schnurr M, Espevik T, Lien E, Fitzgerald KA, Rock KL, Moore KJ, Wright SD, Hornung V, Latz E (2010) NLRP3 inflammasomes are required for atherogenesis and activated by cholesterol crystals. Nature 464(7293):1357–1361
22. Halle A, Hornung V, Petzold GC, Stewart CR, Monks BG, Reinheckel T, Fitzgerald KA, Latz E, Moore KJ, Golenbock DT (2008) The NALP3 inflammasome is involved in the innate immune response to amyloid-beta. Nat Immunol 9(8):857–865
23. Hafner-Bratkovic I, Gaspersic J, Smid LM, Bresjanac M, Jerala R (2008) Curcumin binds to the alpha-helical intermediate and to the amyloid form of prion protein—a new mechanism for the inhibition of PrP(Sc) accumulation. J Neurochem 104(6):1553–1564
24. Hafner-Bratkovic I, Bester R, Pristovsek P, Gaedtke L, Veranic P, Gaspersic J, Mancek-Keber M, Avbelj M, Polymenidou M, Julius C, Aguzzi A, Vorberg I, Jerala R (2011) Globular domain of the prion protein needs to be unlocked by domain swapping to support prion protein conversion. J Biol Chem 286(14):12149–12156
25. Hafner-Bratkovic I, Gaedtke L, Ondracka A, Veranic P, Vorberg I, Jerala R (2011) Effect of hydrophobic mutations in the H2–H3 subdomain of prion protein on stability and conversion in vitro and in vivo. PLoS ONE 6(9):e24238
26. Gaspersic J, Hafner-Bratkovic I, Stephan M, Veranic P, Bencina M, Vorberg I, Jerala R (2010) Tetracysteine-tagged prion protein allows discrimination between the native and converted forms. FEBS J 277:2038–2050
27. Avbelj M, Hafner-Bratkovic I, Jerala R (2011) Introduction of glutamines into the B2–H2 loop promotes prion protein conversion. Biochem Biophys Res Commun 413(4):521–526
28. Franken KL, Hiemstra HS, van Meijgaarden KE, Subronto Y, den Hartigh J, Ottenhoff TH, Drijfhout JW (2000) Purification of his-tagged proteins by immobilized chelate affinity chromatography: the benefits from the use of organic solvent. Protein Expr Purif 18(1):95–99
29. Bocharova OV, Breydo L, Parfenov AS, Salnikov VV, Baskakov IV (2005) In vitro conversion of full-length mammalian prion protein produces amyloid form with physical properties of PrP(Sc). J Mol Biol 346(2):645–659
30. Baskakov IV, Legname G, Baldwin MA, Prusiner SB, Cohen FE (2002) Pathway complexity of prion protein assembly into amyloid. J Biol Chem 277(24):21140–21148
31. Qi Y, Wang JK, McMillian M, Chikaraishi DM (1997) Characterization of a CNS cell line CAD, in which morphological differentiation is initiated by serum deprivation. J Neurosci 17(4):1217–1225
32. Glunde K, Guggino SE, Solaiyappan M, Pathak AP, Ichikawa Y, Bhujwalla ZM (2003) Extracellular acidification alters lysosomal trafficking in human breast cancer cells. Neoplasia 5(6):533–545
33. Andreoletti O, Berthon P, Levavasseur E, Marc D, Lantier F, Monks E, Elsen JM, Schelcher F (2002) Phenotyping of protein-prion (PrPsc)-accumulating cells in lymphoid and neural tissues of naturally scrapie-affected sheep by double-labeling immunohistochemistry. J Histochem Cytochem 50(10):1357–1370
34. Novitskaya V, Bocharova OV, Bronstein I, Baskakov IV (2006) Amyloid fibrils of mammalian prion protein are highly toxic to cultured cells and primary neurons. J Biol Chem 281(19):13828–13836
35. Stewart CR, Stuart LM, Wilkinson K, van Gils JM, Deng J, Halle A, Rayner KJ, Boyer L, Zhong R, Frazier WA, Lacy-Hulbert A, El Khoury J, Golenbock DT, Moore KJ (2010) CD36 ligands promote sterile inflammation through assembly of a Toll-like receptor 4 and 6 heterodimer. Nat Immunol 11(2):155–161
36. Bacot SM, Lenz P, Frazier-Jessen MR, Feldman GM (2003) Activation by prion peptide PrP106-126 induces a NF-kappaB-driven proinflammatory response in human monocyte-derived dendritic cells. J Leukoc Biol 74(1):118–125
37. Spinner DS, Cho IS, Park SY, Kim JI, Meeker HC, Ye X, Lafauci G, Kerr DJ, Flory MJ, Kim BS, Kascsak RB, Wisniewski T, Levis WR, Schuller-Levis GB, Carp RI, Park E, Kascsak RJ (2008) Accelerated prion disease pathogenesis in Toll-like receptor 4 signaling-mutant mice. J Virol 82(21):10701–10708
38. Chang J, Yang L, Kouadir M, Peng Y, Zhang S, Shi F, Zhou X, Yin X, Zhao D (2012) Antibody-Mediated Inhibition of Integrin alpha5-beta1 Blocks Neurotoxic Prion Peptide PrP(106–126)-Induced Activation of BV2 Microglia. J Mol Neurosci 48(1):248–252
39. Shi F, Yang L, Kouadir M, Yang Y, Wang J, Zhou X, Yin X, Zhao D (2012) The NALP3 inflammasome is involved in neurotoxic prion peptide-induced microglial activation. J Neuroinflamm 9:73
40. Petrilli V, Papin S, Dostert C, Mayor A, Martinon F, Tschopp J (2007) Activation of the NALP3 inflammasome is triggered by

low intracellular potassium concentration. Cell Death Differ 14(9):1583–1589
41. Legname G, Baskakov IV, Nguyen HO, Riesner D, Cohen FE, DeArmond SJ, Prusiner SB (2004) Synthetic mammalian prions. Science 305(5684):673–676
42. Wang F, Wang X, Yuan CG, Ma J (2010) Generating a prion with bacterially expressed recombinant prion protein. Science 327: 1132–1135
43. Makarava N, Kovacs GG, Bocharova O, Savtchenko R, Alexeeva I, Budka H, Rohwer RG, Baskakov IV (2010) Recombinant prion protein induces a new transmissible prion disease in wild-type animals. Acta Neuropathol 119(2):177–187
44. Kim JI, Cali I, Surewicz K, Kong Q, Raymond GJ, Atarashi R, Race B, Qing L, Gambetti P, Caughey B, Surewicz WK (2010) Mammalian prions generated from bacterially expressed prion protein in the absence of any mammalian cofactors. J Biol Chem 285(19):14083–14087
45. Silveira JR, Raymond GJ, Hughson AG, Race RE, Sim VL, Hayes SF, Caughey B (2005) The most infectious prion protein particles. Nature 437(7056):257–261
46. Masters SL, Dunne A, Subramanian SL, Hull RL, Tannahill GM, Sharp FA, Becker C, Franchi L, Yoshihara E, Chen Z, Mullooly N, Mielke LA, Harris J, Coll RC, Mills KH, Mok KH, Newsholme P, Nunez G, Yodoi J, Kahn SE, Lavelle EC, O'Neill LA (2010) Activation of the NLRP3 inflammasome by islet amyloid polypeptide provides a mechanism for enhanced IL-1beta in type 2 diabetes. Nat Immunol 11(10):897–904
47. Sharp FA, Ruane D, Claass B, Creagh E, Harris J, Malyala P, Singh M, O'Hagan DT, Petrilli V, Tschopp J, O'Neill LA, Lavelle EC (2009) Uptake of particulate vaccine adjuvants by dendritic cells activates the NALP3 inflammasome. Proc Natl Acad Sci USA 106(3):870–875
48. Prinz M, Heikenwalder M, Schwarz P, Takeda K, Akira S, Aguzzi A (2003) Prion pathogenesis in the absence of Toll-like receptor signalling. EMBO Rep 4(2):195–199
49. Brown DR, Schmidt B, Kretzschmar HA (1996) Role of microglia and host prion protein in neurotoxicity of a prion protein fragment. Nature 380(6572):345–347
50. Brown DR (1999) Prion protein peptide neurotoxicity can be mediated by astrocytes. J Neurochem 73(3):1105–1113
51. Raeber AJ, Race RE, Brandner S, Priola SA, Sailer A, Bessen RA, Mucke L, Manson J, Aguzzi A, Oldstone MB, Weissmann C, Chesebro B (1997) Astrocyte-specific expression of hamster prion protein (PrP) renders PrP knockout mice susceptible to hamster scrapie. EMBO J 16(20):6057–6065
52. Walsh DT, Betmouni S, Perry VH (2001) Absence of detectable IL-1beta production in murine prion disease: a model of chronic neurodegeneration. J Neuropathol Exp Neurol 60(2):173–182
53. Tixador P, Herzog L, Reine F, Jaumain E, Chapuis J, Le Dur A, Laude H, Beringue V (2010) The physical relationship between infectivity and prion protein aggregates is strain-dependent. PLoS Pathog 6(4):e1000859
54. Falsig J, Julius C, Margalith I, Schwarz P, Heppner FL, Aguzzi A (2008) A versatile prion replication assay in organotypic brain slices. Nat Neurosci 11(1):109–117
55. Beringue V, Demoy M, Lasmezas CI, Gouritin B, Weingarten C, Deslys JP, Andreux JP, Couvreur P, Dormont D (2000) Role of spleen macrophages in the clearance of scrapie agent early in pathogenesis. J Pathol 190(4):495–502
56. Tal Y, Souan L, Cohen IR, Meiner Z, Taraboulos A, Mor F (2003) Complete Freund's adjuvant immunization prolongs survival in experimental prion disease in mice. J Neurosci Res 71(2):286–290